How to best estimate the viscosity of lipid bilayers

Vladimir Adrien, Gamal Rayan, Ksenia Astafyeva, Isabelle Broutin, Martin Picard, Patrick Fuchs, Wladimir Urbach, Nicolas Taulier

Journal Pre-proof

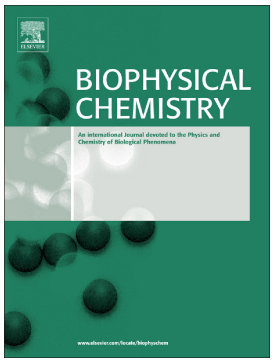

How to best estimate the viscosity of lipid bilayers

Vladimir Adrien, Gamal Rayan, Ksenia Astafyeva, Isabelle Broutin, Martin Picard, Patrick Fuchs, Wladimir Urbach, Nicolas Taulier

PII: S0301-4622(21)00215-5

DOI: https://doi.org/10.1016/j.bpc.2021.106732

Reference: BIOCHE 106732

To appear in: *Biophysical Chemistry*

Received date: 16 August 2021

Revised date: 19 October 2021

Accepted date: 19 November 2021

Please cite this article as: V. Adrien, G. Rayan, K. Astafyeva, et al., How to best estimate the viscosity of lipid bilayers, *Biophysical Chemistry* (2021), https://doi.org/10.1016/j.bpc.2021.106732

How to Best Estimate the Viscosity of Lipid Bilayers

Vladimir Adrien[1,2,3], Gamal Rayan[1,1,*] gamal_rayan@hotmail.com, Ksenia Astafyeva[1], Isabelle Broutin[2], Martin Picard[4], Patrick Fuchs[5,6], Wladimir Urbach[1,7] & Nicolas Taulier[7]

[1]Laboratoire de Physique de l'École Normale Supérieure, ENS, Université PSL, CNRS, Sorbonne Université, Université de Paris, F-75005 Paris, France.

[2]Université de Paris, CNRS, Laboratoire CiTCoM, 75006, Paris, France.

[3]Sorbonne Université, AP-HP Department of Psychiatry, Hôpital Saint-Antoine, Paris FR

[4]Université de Paris, Laboratoire de Biologie Physico-Chimique des Protéines Membranaires, CNRS UMR 7099, F-75005 Paris, France & Institut de Biologie Physico-Chimique, Fondation Edmond de Rothschild pour le développement de la recherche Scientifique, F-75005 Paris, France.

[5]Sorbonne Université, Ecole Normale Supérieure, PSL University, CNRS, Laboratoire des Biomolécules (LBM), 75005, Paris, France.

[6]Université de Paris, UFR Sciences du Vivant, 75013, Paris, France.

[7]Sorbonne Université, CNRS, INSERM, Laboratoire d'Imagerie Biomédicale, LIB, F-75006 Paris, France.

[*]Corresponding author.

ABSTRACT

The viscosity of lipid bilayers is a property relevant to biological function, as it affects the diffusion of membrane macromolecules. To determine its value, and hence portray the membrane, various literature-reported techniques lead to significantly different results. Herein we compare the results issuing from two widely used techniques to determine the viscosity of membranes: the Fluorescence Lifetime Imaging Microscopy (FLIM), and Fluorescence

[1] Current Address. Product Development, Frontida BioPharm, Inc. Philadelphia, PA 19124.

inserted into the membrane to the macroscopic viscosity of a fluid. Whereas FRAP measures molecular diffusion coefficients. This approach is based on a hydrodynamic model connecting the mobility of a membrane inclusion to the viscosity of the membrane.

We show that:

- The first method is very sensitive to local changes in viscosity; however, most often it would only provide the viscosity of the hydrophobic part of the membrane.
- The membrane viscosity is adequately estimated when the hydrodynamic model approach is applied to the mobility of micrometric size membrane inclusion but not for nanometric size inclusions such as lipids or proteins. In this case, the calculated value extracted from the same hydrodynamic model characterizes the interaction of the given nano-inclusion with the bilayer instead of the bilayer viscosity.

This article emphasizes the pitfalls to be avoided and the rules to be observed in order to obtain a value of the bilayer viscosity that characterizes the bilayer instead of interactions between the bilayer and the embedded probe.

Key words: lipids; bilayers; viscosity; diffusion; fluorescence; FLIM; FRAP.

INTRODUCTION

Lipid bilayers are two dimensional fluids, forming the basic architecture of cellular membranes. They provide support to numerous membrane proteins, which need to move within this two - dimensional medium to fulfill their function [1]. Protein diffusion strongly depends on the membrane viscosity and variations in this parameter have been implicated in several diseases [2]. While there is no easy experimental technique to directly measure the bilayer viscosity, various methods provide estimation in an indirect, yet simple manner.

A first approach combines fluorescence lifetime imaging microscopy (FLIM) with the use of specific fluorescent rotors [3-5] to derive bilayer viscosity. These molecular rotors consist of two parts rotating around a simple atomic bond [5-7]. They experience two types of fluorescence

fluorophores while the second one is due to the rotor movement triggered by the absorption, then the release of a photon. This rotating movement derived from the measurement of the fluorescence decay [6, 7] can generally be fitted by a single exponential decay characterizing a fluorescence lifetime. When a rotor is solubilized into a fluid, the viscosity of this fluid can be correlated to the fluorescence lifetime of the rotor, due to its interaction with local environment [7-9]. Thus using liquids of known viscosities one can correlate different fluorescence lifetimes of a molecular rotor to different viscosity values. Once this is established, by simply measuring the fluorescence decay time, τ, one can derive the macroscopic viscosity of the medium in which the rotor is inserted. In other words, the viscosity value can be derived theoretically from local interaction of a molecular rotor with its environment. Moreover, for some molecular rotors the fluorescence lifetime also depends on other parameters such as temperature [10].

A second, more popular, method connects molecular diffusion coefficients to bilayer viscosity. Such hydrodynamic approach models the membrane as a two-dimensional Newtonian fluid of viscosity μ_m and thickness h embedded in a three-dimensional Newtonian solution (Figure 1).

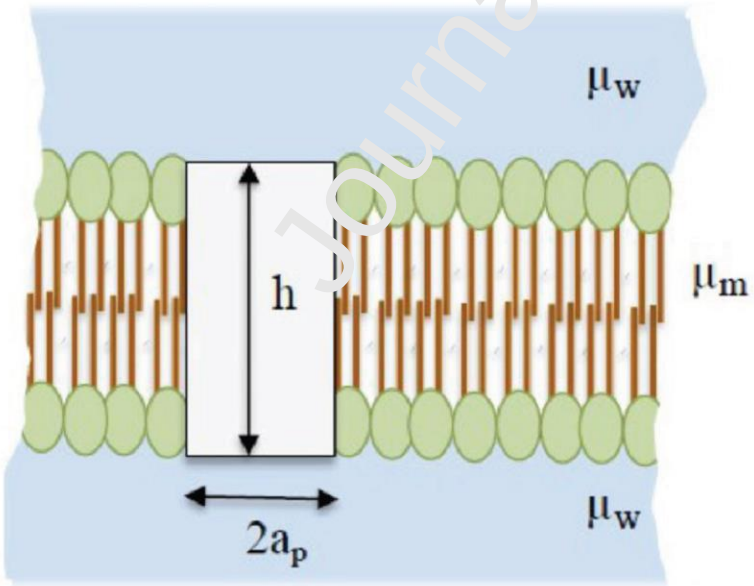

Figure 1. Hydrodynamic model. A cylindrical particle of radius a_p and height h embedded in a lipid bilayer (viscosity μ_m) surrounded by aqueous phases of viscosity μ_m. The system is characterized by the dimensionless constant $\varepsilon = 2a_p \times \mu_w/(h\mu_m)$.

The Saffman-Delbrück model [11] considers an inclusion as an object of lipophilic lateral radius a_p, and length h equal to the membrane thickness. This model is valid as long as the reduced radius $\varepsilon = 2a_p \times \mu_w/h\mu_m \ll 1$. Hughes *et al.* [12] have developed a model without this limitation, but due to its complexity it was scarcely employed. In 2008 Petrov and Schwille [13] provided a tractable equation representing a highly accurate approximation of the model of Hughes *et al.* The measurement of diffusion coefficients is straightforward and uses fluorescence techniques such as single particle tracking (SPT) [14], fluorescence correlation spectroscopy (FCS) [15] or fluorescence recovery after photobleaching (FRAP) [16, 17]. There are a few other and less popular methods that will not be described here [18-21]. It is still unclear how reliable these are in the derivation of membrane viscosities, in particular if they lead to the same viscosity value or at least to the same order of magnitude for a given system.

In the present article, we used literature data that we have completed with our own experimental values to stress out the existing discrepancy in viscosity values for DOPC membranes, also observed in other lipid membranes. We discussed the reasons of these discrepancies based on the two most common methods of measurements: FLIM and FRAP. We further used liposomes composed of DPhPC/DPPC to create micro-domains [22, 23] and compared the diffusion of these micro-domains with the diffusion of a small probe. Overall, we showed that FRAP experiments and the hydrodynamic model provide a correct membrane viscosity but only when applied to the mobility of micron size inclusions, whereas FLIM experiments are reproducible and very sensitive to small changes in bilayer properties but do not provide the exact value of the bilayer viscosity.

Finally, we emphasized the traps to be avoided and the rules to be observed in order to obtain a value of the bilayer viscosity, the one that characterizes the bilayer rather than interactions between the bilayer and the embedded probe.

Lipids and probes.

The lipids:

18:1-DOPC [1,2-dioleoyl-sn-glycero-3-phosphocholine]

16:0-DPhPC [1,2-diphytanoyl-sn-glycero-3-phosphocholine]

14:0-PE-NBD [1,2-dimyristoyl-sn-glycero-3-phosphoethanolamine-N-(7-nitro-2-1,3-benzoxadiazol-4-yl) (ammonium salt)];

14:0-6-PE-NBD [1-myristoyl-2-{6-[(7-nitro-2-1,3-benzoxadiazol-4-yl)amino]hexanoyl}-sn-glycero-3-phosphoethanolamine]

DID-C_{18} [1,1'--dioctadecyl-3,3,3',3'- tetramethylindodicarbocyanine, 4-chlorobenzenesulfonate salt]

DIL- C_{18} [1,1'-dioctadecyl-3,3,3' ,3'-tetramethylindocarbocyanine perchlorate]

were purchased from Avanti Polar Lipids (Alabaster, USA) and used as received.

The molecular rotor, BODIPY-C_{10} [meso-4-decyloxyphenyl-4,4-difluoro-4-bora-3a,4a-diaza-s-indacene] was generously provided by Dr. M. K. Kuimova [24].

Transmembrane Proteins

Alexa 488-labeled TolC and OprM are trimeric 12-stranded α/β barrels, comprising an α-helical periplasmic tunnel embedded in the outer membrane of *Escherichia coli* and *Pseudomonas aeruginosa*, respectively, by a contiguous β-barrel channel [25]. OprM was purified according to Daury *et al.* [26] and the same protocol was applied to TolC in order to end in the same detergent quantity for both proteins (0.9% w/v β-OG). In all of our experiments the lipid to dye ratio was around 1000:1 for proteo-GUVs or BODIPY-C_{10} GUVS and of 200:1 for GUVs with labelled lipids.

Formation of Giant Unilamellar Vesicles.

GUVs were electroformed on indium-tin oxide coated glass slides (Delta-Technologies) of sheet resistance 20-25 Ω as described previously [27-30]. The fluorophore was introduced in the lipid mixture, which was dried under vacuum prior to electroformation. In order to avoid dimer

made of pure DOPC, or a mixture of DPhPC/DPPC 1/1 (mol/mol). GUVs with embedded membrane protein were formed by osmotic shock [31]. DPhPC/DPPC GUVs were filled with an aqueous solution containing 300 mM of sucrose and were observed in an equi-osmolar aqueous solution containing 225 mM of glucose and 75 mM of sucrose, following the protocol of Petrov et al [23]. DOPC GUVs containing a small dye or a protein were filled respectively, with 200 mM and 100 mM of sucrose while the outer aqueous solution contained 220 or 100 mM of glucose. The inside and outside solution also contained 100 mM NaCl and 50 mM Tris buffer (pH 8) when the protein was TolC.

Fluorescence Lifetime Imaging Microscopy (FLIM)

We have used BODIPY-C_{10} to measure the viscosity of the bilayers by FLIM [30]. Two-photon excitation was performed at 800 nm with a Vision II femtosecond laser (Coherent Inc.) on a Leica SP8 SMD system with an inverted DMI6000 microscope and a 63 x NA 1.4 objective. We evaluated the data only if the GUV remained in the analyzed frame during acquisition. The fluorescence decays, measured by time-correlated single-photon counting (TCSPC), were recorded at 515 nm using a band-pass filter (500 – 550 nm). The image format was set to 512 x 512 pixels to get images of an entire GUV while keeping the pixel size small. A typical FLIM fluorescence decay curve, of a BODIPY-C_{10} inserted into a GUV made of a DPhPC/DPPC bilayer, is displayed in Figure 2. Some authors have reported a bi-exponential decay, either in the gel phase or in a fluid phase composed of several lipid species [9, 32]. In this study only a mono-exponential decay was observed for all fluid phases. Thus, all the fluorescence decays were fitted by a mono-exponential model with a characteristic decay time, τ, using the Levenberg-Marquardt algorithm in TRI2 Software Version 2.7, provided by the Gray Institute for Radiation Oncology and Biology [33]. Hosny *et al.* [34] have established a calibration curve relating the fluorescence lifetime, τ, of BODIPY-C_{10} to the bulk viscosities, μ, of different liquid mixtures of ethanol and glycerol, in which BODIPY-C_{10} was solubilized. In the range of 7.7 – 1140 mPa.s this calibration was well fitted by the Förster-Hoffmann equation [6, 35, 36].

where k is the radiative rate constant, α and z are constants. According to the fit of Wu *et al.* [9] $\alpha \approx 0.5403$ and $\ln(z/k) \approx 4.55$. Furthermore, Vyšniauskas *et al.* [10] determined that this linear fit is valid in the temperature range 278 - 334 K.

To determine the bilayer viscosity, μ_m, we used Equation 1 where τ was the average of fluorescence decay time measured on about 10 GUVs for each GUV system.

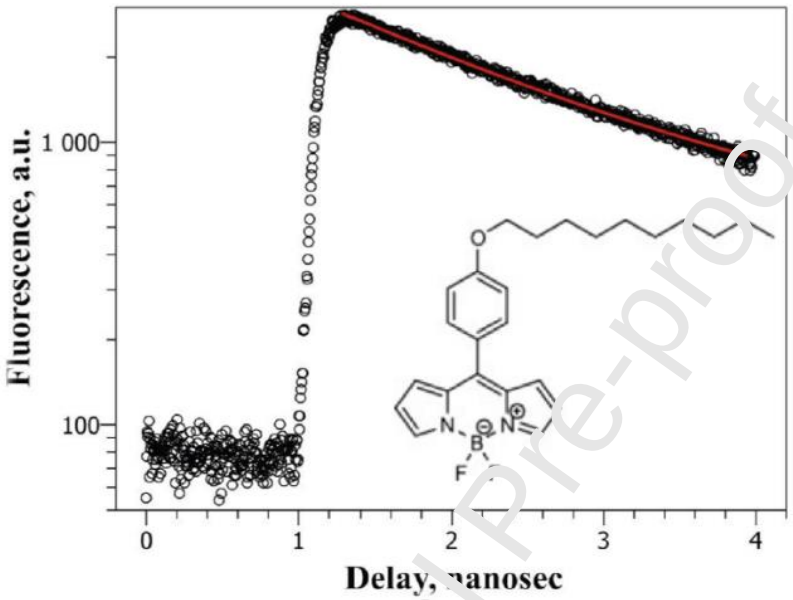

Figure 2. The BODIPY-C_{10} molecular structure and, in semi-log, the typical decrease of the FLIM intensity in the fluid phase of GUV DPhPC/DPPC. The red line is an adjustment to the experimental results confirming the monoexponential decay with the fluorescence lifetime $\tau = 1.84 \pm 0{:}04$ ns. The viscosity of the bilayer, $\mu_m = 243 \pm 10$ mPa.s, was derived using Equation 1 after averaging fluorescence lifetimes obtained on 10 GUVs for two different samples.

In all experiments dye aggregation was prevented by using a lipid/BODIPY-C_{10} molar ratio of 1000 [9]. The absence of aggregation was further confirmed by the facts that fluorescence lifetime was independent of the emission wavelength and that the emission spectrum was centered on 520 nm. It would have been 650 - 700 nm in the presence of aggregated BODIPY-C_{10} [9].

Diffusion coefficients of BODIPY-C_{10} in GUV bilayers were measured by FRAP at $T = 296 \pm 1$ K using a confocal microscope enclosed in a protective box to minimize air convection which would otherwise induce water flow within the sample. For these measurements we only used GUVs with a diameter of at least 25 µm. During each measurement, the GUV was slightly aspirated and manipulated by a micropipette in order to keep it motionless, away from the bottom of the Petri dish and entirely surrounded by solvent [37].

The focus was kept on top of the GUV and the bleached region of interest (ROI) was circular with a radius r. We made sure that the GUV radius was at least 5 µm larger than the *r*. To measure a diffusion coefficient, *D*, we used at least 15 GUVs varying the r from 5 to 20 µm, with a 2.5 µm increment. The scanning frequency was set at either 400 or 700 Hz depending on the signal-to-noise ratio. In the case of DPhPC/DPPC GUVs, the fluorescence recovery curve was excluded from analysis if a non-fluorescent gel domain was observed to cross the ROI during the measurement. The fluorescence recovery curves, *f(t)*, were fitted with the equation [38]:

$$f(t) = \frac{I(t) - I_0}{I_p - I_0} = e^{\frac{-2t}{\tau}}\left[J_0\left(\frac{2t}{\tau}\right) + J_1\left(\frac{2t}{\tau}\right)\right] \qquad (2)$$

Where *I(t)* is the fluorescence intensity at time *t*, I_0 the minimal intensity just after the bleach, I_p the intensity at the stationary state once the fluorescence has recovered, and J_0 and J_1 the Bessel functions of the first kind. The characteristic mean recovery time, $<\tau>$, was the average of fluorescence decay times, τ, measured on about 10 GUVs for each *r* value.

The resulting $<\tau>$ values were plotted versus r^2. Finally, the *D* value was deduced from the slope of a linear regression (Figure 3) following the equation:

$$D = \frac{r^2}{4 < \tau >} \qquad (3)$$

The observed linear variation of $<\tau>$ versus r^2 confirmed that the diffusion was Brownian. It also showed that artifacts due to GUV curvature are negligible [38].

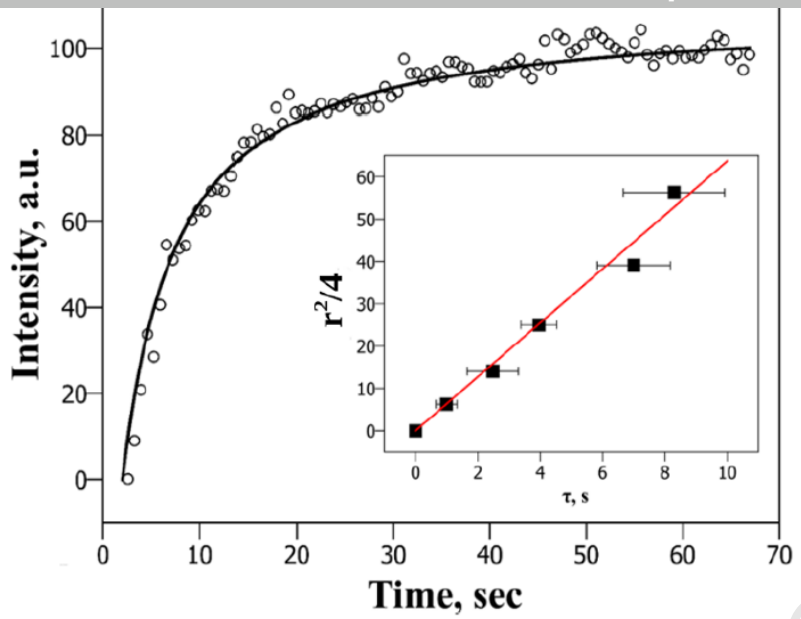

Figure 3. Typical FRAP results. Intensity recovery due to the diffusion of BODIPY-C_{10} in a GUV made of 1:1 (mol:mol) DPPC/DPPC bilayer. Here the GUV radius r_{GUV} = 25 µm and the ROI radius r = 5 µm. The fit of experimental data by Equation 2 (black solid line) led to the characteristic decay time of τ = 4.0 ± 0.2 s. Inset: the variation of $r^2/4$ versus the averaged characteristic decay times $\langle\tau\rangle$ determined on 15 GUVs. The linear behavior is the proof of the Brownian motion of the probe, and the slope of the linear fit (red line) yielded the diffusion coefficient D = 5.4 ± 0.4 µm^2/s.

Knowing the D value, the bilayer viscosity μ_m is derived using either the Saffman-Delbrück (SD) [11] equation:

$$D = \frac{k_B T}{4\pi h \mu_m}\left[ln\left(\frac{2}{\varepsilon}\right) - \gamma\right] \qquad (4)$$

where γ = 0.577 is the Euler constant, $\varepsilon = 2a_p \times \mu_w/(h\mu_m)$, a_p is the radius of the hydrophobic part of diffusing probe, h is the length of the hydrophobic part of the probe (which can be different from the membrane hydrophobic thickness) and μ_w the viscosity of the surrounding aqueous phase. Equation (4) is valid if $\varepsilon \ll 1$, whereas the equation of Petrov and Schwille [13] is valid for all ε values:

$$D = \frac{k_B T}{4\pi h \mu_m} \times \frac{ln\left(\frac{2}{\varepsilon}\right) - \gamma + \frac{\varepsilon^2}{\pi} - \frac{\varepsilon^2}{2} ln\left(\frac{\varepsilon}{2}\right)}{1 - \frac{\varepsilon^3}{\pi} ln\left(\frac{2}{\varepsilon}\right) + \frac{c_1 \varepsilon^{b_1}}{1 + c_2 \varepsilon^{b_2}}} \quad (5)$$

where the values of constants are: c_1 = 0.73761, c_2 = 0.52119, b_1 = 2.74819, and b_2 = 0.61465 [16].

We would like to emphasize that in Equations (4) and (5) μ_m represents the 3D viscosity of the bilayer (in Pa.s). Indeed, in their seminal paper Saffman and Delbrück [11] considered a cylindrical inclusion, of radius a_p and of length h, embedded within a bilayer of same thickness. Even though since then several authors [39-41] preferred to use $\eta = h\mu_m$, the so-called "2D viscosity" of the bilayer, we stick to the bulk value, μ_m, which can be directly compared to the viscosity of common fluids.

RESULTS AND DISCUSSION

Since the value of a bilayer viscosity is characteristic of the membrane it should be independent of inclusion size, and it should not be affected by the addition of a fluorescent probe. The later has been corroborated by molecular dynamics simulations [42, 43], which show that the addition of a probe has a minimal effect on bilayer viscosity. An identical value should be derived for a bilayer viscosity regardless of the size of a diffusing inclusion embedded into this bilayer. Clearly, this is not what is observed when considering results taken from the literature as well as from our experiments (see Table 1). In order to simplify the discussion that follows, we will consider only the viscosities of GUVs prepared from two different types of bilayers: pure DOPC, and DPhPC/DPPC.

Table 1. Viscosities of the GUV bilayers of DOPC (of membrane thickness h = 3.7 ± 0.2 nm and of hydrophobic thickness 2.7 nm) extracted from the literature as well as the results obtained in this work. The first column lists the probes used. The second column gives the values of the diffusion coefficient of the probe in the bilayer; $\mu(x)$ indicates the value of the viscosity according to whether one fixes $x = h$ or $h/2$. a_p indicates the radius

[49]; the *h* values were roughly estimated by authors; $I_{hydrophobic}$ is the maximum length of the hydrophobic part of the probe. FLIM: Fluorescence Lifetime Imaging; FRAP: Fluorescence Recovery After Photobleaching, (2f)-FCS: (dual-focus)-Florescence Correlation Spectroscopy; TRFA: time-resolved fluorescence anisotropy.

PROBE	*D* ($\mu m^2 s^{-1}$)	*μ(h/2)* (mPa.s)	*μ(h)* (mPa.s)	a_p (nm)	$l_{hyrophobic}$ (nm)	T (K)	Method	Year	Reference
BODIPY-C_{12}	—	—	222*	0.6		295	FLIM	2013	9
BODIPY-Cholesterol	—	—	232	0.5		295	TRFA	2009	44
BODIPY-C_{10}	—	—	214	0.6		295	FLIM	2020	This work
14:0-6-PE-NBD	7.9	127	65	0.5	1.75	295	FRAP	2020	This work
14:0-PE-NBD	7.4	137	75	0.5	1.75	295	FRAP	2020	This work
18:0-PE-NBD	8.6	115	56	0.5	2.25	295	FRAP	2020	This work
DOPC	9.3	104	51	0.5	1.85	296	NMR	2003	45
BODIPY-C_{10}	10.5	90	42	0.5	1.25	293	FCS	2015	32
BODIPY-C_{12}	14.6	60	27	0.5	1.5	ROOM	2fFCS	2013	9
BODIPY-C_8	7.8	130	63	0.5	1	298	FCS	2006	46
DiD-C_{18}	10	137	69	0.8	2.25	296	FCS	2012	47
DiI-C_{18}	6.5	237	118	0.3	2.25	ROOM	FCS	2006	48
TolC-Alexa 488	2.4	—	255	2	3.4	295	FRAP	2020	This work
OprM-Alexa488	1.1	—	530	2	3	295	FRAP	2020	This work

(*) This value was estimated at T = 295K using experimental determination by FLIM of μ_m variation with temperature in reference [9].

1) Viscosity of DOPC bilayers.

a) Results from our FLIM experiments and from literature using lipid-like probes

DOPC is a widely used lipid as witnessed by more than 200 publications over the past several years, in which this model lipid has been used. Since a DOPC bilayer exhibits a gel-liquid transition at T_m = 256 K [50], it exists in a liquid-phase at room temperature. A quick inspection of values in Table 1 reveals a large dispersion of the viscosity values.

Our FLIM measurements, performed at 295K on DOPC GUVs containing embedded BODIPY-C_{10}, exhibited only one characteristic time $\tau = 1.72 \pm 0.04$ ns, that led to a DOPC bilayer

deduced from Wu *et al*. results [9] who used the same technique. These values are of the same order of magnitude as those determined by Ariola *et al.* [44] who used time-resolved fluorescence anisotropy (TRFA) to measure the rotational diffusion of BODIPY-cholesterol. From the observed rotation times, they derived viscosities of 232 ± 7 mPa.s. From the above values the mean viscosity value of DOPC bilayer is $<\mu_m>$ = 223 ± 6 mPa.s.

In the rest of the Table, the viscosity values that are deduced from diffusion measurements of membrane objects are much more dispersed, varying from 27 to 630 mPa.s.

b) Possible reasons for the dispersion of experimental values of μ_m deduced from diffusion of lipid-like probes.

The first reasons to be considered are the correct choice of h and a_p values as well as the reproducibility of GUVs properties. Indeed Equation 4 was obtained by considering the diffusion of a cylinder of radius a_p and height h in a bilayer. The parts outside the bilayer can be neglected as long as $\mu_w l_w < \mu_m h$ where l_w is the height of the cylinder in the solvent. When using Equation 4 for a molecular object, it is, therefore, a question of modeling the diffusing molecule by an equivalent cylinder. Thus a lipid will be modeled by a cylinder of radius $a_p \approx$ (average area per lipid/π)$^{0.5}$ while a protein will be, as a first approximation, modeled by a cylinder whose lateral area (the one on which the viscous force is exerted) is equal to the hydrophobic surface of the protein.

The h value can be another reason explaining the dispersion of viscosity values. One of the problems encountered in deriving the viscosity from the mobility values is the choice definition of the "h" value (see Figure 1). For lipid-like dyes, there is often a low dependence of the translational diffusion coefficient on the length of the lipids [51-54]. According to different authors [55] this could be due to the fact that when the probe moves in a monolayer of a bilayer and if the inter-monolayer friction strongly couples the movement of the probe to the adjacent monolayer, then for all practical purposes, the probe can be treated as a cross-layer particle. Consequently, authors cited in Table 1 considered that the dimensionless radius, ε, must be

However-*in vitro* and *in silico* studies have shown the possibility of chain folding, i.e. finding the methyl group of a given chain near the head group region of the same monolayer [56]. Thus, by generalizing, one could suggest that whatever the length of the carbon chain, *h/2* instead of the membrane thickness *h* should be used for ε, even if the hydrophobic length of the lipid tracers exceeds the thickness of a DOPC monolayer (1.8 nm) [57].

In Table 1 we calculated the viscosity values for *h* and *h/2*. In both cases a large error (30%) is observed in the μ_m values obtained from the mobilities of objects; for instance in the sixth row of Table 1 the corresponding mean values are $<\mu_m\ (h)> = 56 \pm 18$ mPa.s and $<\mu_m\ (h/2)> = 115 \pm 34$ mPa.s.

The dispersion of *D* values could also be due to the fact that even if they are made by a single method, GUVs are rarely identical and some of them may be slightly more floppy than others. Experiments have however shown that the mobility of molecules of quasi-cylindrical shape does not depend on the tension of the membrane [58].

Before ending this paragraph let us make clear that two different approaches model the mechanism of diffusion of lipids in bilayers: the theory of free volume [59], where lipids diffuse by thermally activated jumps if there is a sufficiently large free volume adjacent to the lipid; and a model which proposes that the diffusion is due to collective lipid movements. Recent experimental work [60, 61] and computer simulations [62] are in favor of the classic lipid movement and the use of Equation 4. However it could still be argued that further research, both experimental and theoretical, is needed to settle this point definitively. This is not the goal of this article. That is why we present below the results obtained from the diffusion of membrane proteins, a system for which most authors accept that Equation 4 applies.

c) Viscosity values deduced from transmembrane protein diffusion

In DOPC GUVs we measured by FRAP the diffusion constants of two transmembrane proteins TolC [63] and OprM [64] (Figure 4). The TolC hydrophobic part consists of a ß-barrel of height $h \approx 3$ nm with hydrophobic residues oriented toward the exterior where they contact the

lateral loops, is between 1.5 and 1.9 nm leading, using equation (4), to viscosity values of $\mu_m \approx 260$ and 250 mPa.s respectively, i.e. an average value of $< \mu_m > \approx 255 \pm 5$ mPa.s.

While the hydrophobic part of TolC is almost cylindrical, that of OprM appears rather triangular, constituted, in the first approximation, of three adjacent planes of height $h = 3$ nm. Including the curved parts connecting the planes, the total hydrophobic surface in contact with the lipids is $S = 10.2h$. The radius of a cylinder having the same lateral surface would be $a_p = 1.6$ nm, leading to $\mu_m \approx 650$ mPa.s. Taking into account the lateral loops then the hydrophobic part of the protein must be enclosed in a cylinder of radius $a_p = 2.0$ nm. This value, certainly overestimated, leads to $\mu_m = 630$ mPa.s. In order to verify this point, we measured the values for the hydrophobic surface of OprM and TolC (see Supporting Information). The values of the corresponding surfaces, embedded in the bilayer are for OprM and TolC $S = 60$ and 54 nm^2 respectively leading to $\mu_m = 650$ and 265 mPa.s therefore on the same order of magnitude as the "naive" approach outlined above".

Whereas the diffusion coefficient of TolC leads to a μ_m value of the same order of magnitude as that obtained by the FLIM experiment, the values extracted from the diffusion coefficient of OprM appear significantly different. This could be due to the difficulty, when the hydrophobic part of the protein is too far from the cylindrical model, of correctly defining the radius of an equivalent cylinder, needed in Equation 4. It appears, therefore, when the hydrophobic part is not too far from that of a cylindrical structure, that FLIM and protein diffusion provide similar values of μ_m.

d) Difficulty of choosing a protein radius.

The choice of the radius value does remain questionable. Numerical simulations suggest that one should rather consider the diffusion of a complex made of a protein with neighboring lipids [65] i.e. an effective protein radius, a_{eff}. It is reasonable to postulate that the number of lipids diffusing with a protein should depend on its hydrophobic domain i.e. the "smoother" the hydrophobic part the smaller the effective radius. Contrary to the TolC hydrophobic part, modeled by a cylinder,

lipid linked to the membrane, originating from the posttranslational modification of its N-terminal cysteines. This additional anchoring, together with the triangular shape of its membrane-embedded domain, could favor a larger lipid-associated corona explaining the lower mobility of OprM. Thus the a_p value of 1.6 nm is probably underestimated. However, the values of a_{eff} remain open questions since, to the best of our knowledge, the structural data indicating the values of the corona radius (i.e. representing the lipids around the protein that are perturbed by the protein) for such proteins remain unavailable. We know however that for aquaporin-0 (AQP0) with a smooth square-like hydrophobic part, the estimated corona radius is of the order of 4 nm [66, 67].

Finally if one assumes that the effective radius of each protein should lead to an average viscosity value determined above from lipid diffusion, $<\mu_s(h/2)> \approx 110$ mPa.s, then it will reciprocally lead to an effective radius for TolC of $a_{eff} = 18$ nm and for OprM of $a_{eff} = 65$ nm. Simulations of the even more irregular hydrophobic part of voltage-gated channel Kv1.2, suggest that lipids diffuse with the protein up to 4 nm from the lipid-protein interface with an irregular distribution following the protein shape [65]. If applied to OprM this would result in an a_{eff} no larger than 6 nm. Thus the above values for a_{eff} appear unlikely.

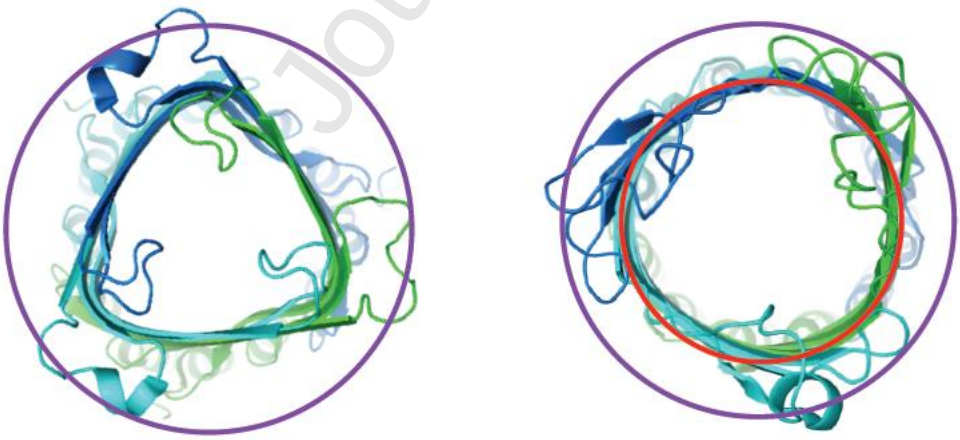

Figure 4. Structures of OprM (left, PDB code3D5K) and TolC (right, 2VDD) viewed from the extracellular side. Their respective ß-barrel presents a different shape, being triangular for OprM and round for TolC. Red and purple circles illustrate the smallest and the largest hydrophobic part as discussed in

An alternative vision would be to consider that even if the neighboring lipids are not strongly bound to the protein, their diffusion is slowed down. The diffusion of proteins would, therefore, probe a local viscosity that differs from that of the bilayer.

The above discussion favors the idea that the "viscosity" of DOPC bilayers extracted from the mobility values of molecular size probes does not characterize the membrane, but rather reflects the interaction of the nano-object with the membrane into which it diffuses and thus depends on the characteristic of the nano-object as well.

Thus, all the results cited suggest abandoning the determination of viscosity using hydrodynamic models, at least as far as nanometric probes are concerned. In the next paragraph, we suggest that the viscosity of membranes could still be estimated correctly by studying the diffusion of micrometric size transmembrane probes using the convenient system of DPhPC/DPPC liposomes.

2) Viscosity of DPhPC/DPPC bilayers.

In what follows we compare the results obtained with the diffusing molecules to those obtained by studying the diffusion of membrane micrometric inclusions. In the temperature range of 153 K up to 393 K DPhPC forms a liquid phase bilayer [68], while DPPC exhibits a gel-liquid transition at T_m = 314 K [69]. Below 308 K an equimolar mixture of DPhPC/DPPC shows coexistence of a gel phase and of a liquid phase mainly composed of DPPC and DPhPC, respectively [22].

After the insertion of BODIPY-C_{10} in GUVs consisting of an equimolar mixture of DPhPC/DPPC, we observed on the GUV surface the presence of several non-fluorescent, diamond-shaped, micrometric regions, while the rest of the surface was fluorescent. According to different authors [22, 23] the overall fluorescent region corresponds to a liquid bilayers phase (mainly composed of DPhPC), whereas non-fluorescent regions are gel phase domains (mainly

diamond-shaped regions and BODIPY-C_{10} are both inclusions moving in the liquid-phase of the GUV. Thus, we should derive the same the viscosity using the same hydrodynamic model. Petrov et al [23] already measured the diffusion of the gel-phase domains (dark micrometric regions) and obtained a value of 580 mPa.s.

When performing FLIM measurements on the latter, we only observed monoexponential decay (such as seen in Figure 2), and therefore concluded that BODIPY- C_{10} is moving inside the large liquid phase region of a GUV.

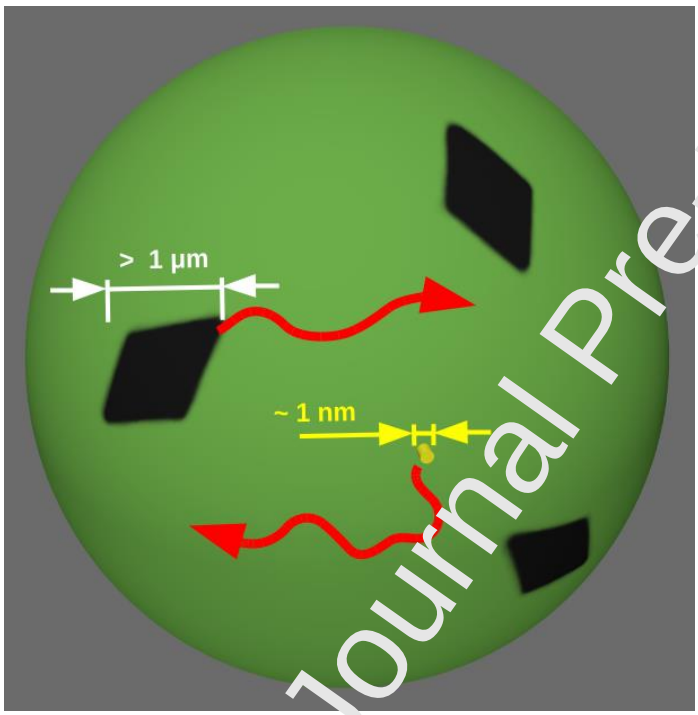

Figure 5. Cartoon (not in scale) of a GUV made of DPPC / DPhPC 1:1 (mol/mol) bilayer. The large fluorescent region (in green) is in liquid phase, whereas the small non-fluorescent domains (in black) are in gel-phase. We followed the diffusion of BODIPY-C_{10} (in yellow, with a diameter of ≈ 1.2 nm) in the liquid phase bilayer, while Petrov et al [23] followed the diffusion of the gel-phase domains (dark micrometric regions).

Our FLIM measurements led to an average fluorescence lifetime $\tau = 1.84 \pm 0.04$ ns for BODIPY-C_{10}, which in turns lead to a bilayer viscosity of $\mu_m = 243 \pm 10$ mPa.s. Using FRAP, we measured

viscosity of the surrounding solution to be μ_w = 0.905 mPa.s at 297 K (see Supporting Information), the lateral radius of BODIPY-C_{10} $a_p \approx 0.62$ nm [32], and h_{BODIPY} = 1.9 nm [70], Equation 4 or 5 leads to the viscosity of the liquid phase of the DPhPC/DPPC bilayer μ_m = 150 ± 10 mPa.s.

Petrov et al. [23] optically monitored the Brownian movements of the non-fluorescent micrometric domains in the gel phase using single raft tracking. From their experiments, the authors obtained a surface viscosity of the liquid phase DPhPC / DPPC bilayer $h\mu_m = (2.2 \pm 0.1).10^{-6}$ m.Pa.s, which corresponds to a viscosity of μ_m = 580 ± 30 mPa.s, twice as large as the FLIM value. This difference could be due to the localization of BODIPY. In DOPC bilayers molecular dynamics simulations have located BODIPY-C_{10} in the hydrophobic part of the bilayer [32]. Thus, if in DPPC membranes, BODIPY-C_{10} also only probes the hydrophobic part of the bilayer, the FLIM experiments would underestimate the viscosity of the bilayer as a whole.

In addition, using the viscosity value they determined, Petrov et al. [23] showed that the theoretical value of the rotational diffusion of microdomains correctly matches their experimentally determined value. The difference of 6% was on the order of the experimental error in their study [23]. In our opinion, these results validate the use of the hydrodynamic model for the determination of membrane viscosity once the mobility of an object of microscopic size is known. While the results obtained with the nanometric probe remain, as indicated above, questionable.

Our observations, as well as the results gathered from the literature, indicate that the information extracted from the diffusion of nanometric objects (using Equation 4 or 5) relates the interaction of the marker/diffusing probe with the bilayer rather than the viscosity of the bilayer itself: each nanometric marker "feels" a different viscosity. This is in contrast with Vaz and Hallmann [71] who suggested that the hydrodynamic model does not apply to lipids but works with nanometric transmembrane objects.

Beyond resolving the latter controversy, our results bear biological significance because modulation of hydrophobic mismatch and local membrane deformation [72], lateral organization [73], curvature [74] or membrane viscosity critically modulate the function of membrane proteins. A most recent and relevant example, is the case of rhomboid intramembrane proteases. They regulate the activity of many key targets by performing enzymatic cleavage within the lipid membrane during interaction with their substrate upon lateral diffusion. Protein-induced membrane deformations can generate new hydrodynamic stresses on the protein-membrane complex leading to a shift in their mobility [75] and it has been suggested that the irregular shape of the transmembrane segments of rhomboid proteases reduces local viscosity, hence accelerating protein diffusion to maximize their catalytic efficiency [76].

4) Suitability of nanometric and micrometric probes for determining membrane viscosity

It seems from the above that biophysical approaches will hardly allow for a universal way to measure viscosity based on the mere diffusion of nanometric probes. Does this consequence make the use of nanometric markers totally inoperative? It depends on the purpose. Often the intrinsic value of the viscosity of a bilayer has little interest. What we may want to determine are variations of the viscosity of a membrane upon imposition of an external stimulus. In this case, it is the relative variation of the diffusion coefficient that is relevant, and the measurements are of interest, provided that the stimulus does not affect the interaction between the nanometric probe and the membrane. On the other hand, it is advisable to be very careful when it is proposed to compare the viscosities of two bilayers made from distinct lipids. The dispersion of the results observed in Table 1 strongly suggests that a variation of 30 % could be insignificant.

For inclusions with a radius significantly larger than the structural details of the membrane (i.e. lipids or proteins) the bilayer can be considered as a continuous liquid slab of viscosity μ_m and the hydrodynamic approach relating the probe mobility to the viscosity of bilayer is then fully justified. For this reason, the viscosity value deduced from the mobility of the gel domains of

conditions are not those of the model. Indeed molecular exchanges between two phases are very likely to occur at the gel-phase interface. On the other hand, one should be sure that multiple domain presence does not increase bilayer viscosity. However for surface fractions of the order of 2 %, the overestimation of the viscosity does not exceed 15 % [77].

In FLIM experiments the characteristic time of fluorescence decay of a molecular rotor is related to the viscosity of the medium in which it is dissolved. This raises the question of precise localization of molecular rotor in lipid bilayers where the physical properties of hydrophobic and hydrophilic parts differ. For example, since the lateral pressure varies significantly between the lipid heads and tails [78] one should expect that the resistance to rotation of a molecular rotor will be different in the hydrophobic region of the lipid bilayer compared with the hydrophilic one. BODIPY-derived moieties have been shown to prefer the polar region of the bilayer [79]. BODIPY probes in tail-labeled lipids have, therefore, a tendency to loop back to the surface perturbing the local lipid order and increasing the area required for a tracer molecule [80].

5) How far can we trust viscosity values determined by FLIM and FRAP?

Each technique has its pros and cons and it is important to bear in mind their limitations when interpreting viscosity values. In this last section we discuss some limitations of viscosity determination using both FLIM and FRAP techniques.

First, there might be a dimensionality issue in FLIM experiments. Indeed, one usually deduces viscosity of a lipid bilayer from a bulk viscosity calibration curve. If the relaxation time of a molecular probe gives the same value in a lipid bilayer as it does in a 3D liquid of some viscosity, then it does not follow that both have the same viscosity. Suppose we decrease the thickness of the fluid in which a FLIM probe is embedded down to molecular scales, like a lipid bilayer, so that the environment can be modeled in two dimensions, it is not obvious that the lifetime will be unchanged. Knowing that decay time gives a value without calibration of what being in a bilayer-like environment means, it is not sure that this value can be mapped to the drag

does not depend on their thickness (down to 5 nm or less). However, it is not clear whether this conclusion holds for thin films made of amphipathic molecules such as lipids, which are intrinsically more anisotropic. To the best of our knowledge, there is no experimental answer to this question and nonetheless articles have been published that relate the 3D viscosity calibration curve to the "viscosity" of the bilayer. Second, the BODIPY- C_{10} is sensitive to the polarity of the solvent and therefore an accurate determination of the viscosity would only be possible if the BODIPY-C_{10} were calibrated in the same polarity environment as in the sample of interest [82]. It could thus be that the ethanol glycerol mixture mentioned here is not the best suited for estimating the viscosity of the bilayers. Anyway our contribution shows that the results extracted from FLIM do not match the viscosity values extracted from the diffusion of microscopic entities, which we believe are the correct viscosites of the bilayer since the hydrodynamics approach makes sense for such mesoscale objects. This discrepancy could be due either to the position of BODIPY in bilayers and/or to the above objection.

Regarding FRAP experiments, there might also be an issue due to mixing different scales. The relationship between the diffusion coefficient and viscosity provided in Equation 4 comes from continuum hydrodynamics; there is no reason to expect it to hold at the molecular level. It is therefore questionable to use a molecular diffusion coefficient determined by FRAP in those equations. One can of course calculate a viscosity, but it remains to be proved if the latter is identical to the viscosity felt by a macroscopic object (for example a lipid domain). The differences between the viscosity values determined using the diffusion of molecules or lipid domains do not mean that the theory or the methods are wrong, but rather that we are examining different properties at different scales.

CONCLUSION

In the literature, there is considerable confusion regarding both the concept of "viscosity" and the interpretation of results obtained from different methods. We believe that this manuscript helps

When one is interested in the transport of nanoprobes, the hydrodynamic approximation is no longer valid and the use of the Saffman Delbrück or Stokes Einstein equations remains questionable. We show in this article that instead of measuring an intrinsic property of the bilayer, the use of nanoprobes tends to characterize the interaction between the bilayer and the diffusing molecule. It is only when the probe is micrometric that the hydrodynamic approximation becomes justified and the use of the Saffman Delbrück or Stokes Einstein relation in deducing the viscosity becomes legitimate.

From the discussion in the last section we conclude-the following points:

• The "viscosity" extracted from the mobility of molecular probes does not characterize the membrane, but rather reflects the interaction of the molecule with the membrane and thus depends on the characteristic of the nano-object as well.

• Consequently, only the mobility of objects of micrometric size should be used to obtain the correct value of the bilayer viscosity.

• The "FLIM approach" most probably does not provide the exact value of bilayer viscosity. This is due to the fact that molecular rotors, such as the BODIPY-C_{10}, mainly probe the viscosity of the hydrophobic part of the bilayer. Despite this, the FLIM technique is reproducible and very sensitive even to small changes in bilayer properties induced for instance by an external stress [34] or a change in bilayer composition [44]. Thus, whenever the absolute value of the bilayer viscosity is not required, it appears that FLIM measurements coupled with the use of molecular rotors is the most robust method to assess a variation in bilayer viscosity.

ACKNOWLEDGEMENTS

This work was supported by Agence Nationale de la Recherche (ANR-12-BSV8-0010-01), the Fondation pour la Recherche Médicale (FRM n.o DGE20111123020), the Cancerople - IdF (n.o 2012-2-EML-04-IC-1), and INCa (Cancer National Institute, n.o 2011-1-LABEL-IC-4). The funding sources had no involvement in the following; study design, data collection, data

publication.

We are grateful to Dr. M. K. Kuimova for the generous gift of BODIPY-C_{10} .

We acknowledge Drs E. Perez, A. Ducruix and D. Hodara for simulating discussions and careful lecture of the manuscript.

V. A. was funded by the Ph.D Program of École Doctorale Frontières du Vivant (FdV) - Programme Bettencourt.

FLIM experiments were performed on the PICT-IBiSA imaging facility with the help of F. Waharte at Institut Curie, Paris, France.

Author Statement
Vladimir Adrien: Investigation, Formal Analysis, Writing-Original Draft preparation **Gamal Rayan:** Writing-Original Draft preparation, Writing-Review & Editing **Ksenia Astafyeva:** Investigation, Writing-Original Draft preparation **Isabelle Broutin:** Writing-Original Draft preparation, Supervision, Resources **Martin Picard:** Investigation, Writing-Original Draft preparation **Patrick Fuchs:** Software, Formal Analysis, Writing-Original Draft preparation, Resources **Wladimir Urbach:** Conceptualization, Methodology, Supervision, Formal Analysis, Resources, Project Administration, Writing-Original Draft preparation, Writing-Review & Editing **Nicolas Taulier:** Methodology, Formal Analysis, Resources, Project Administration, Writing-Original Draft preparation

Declaration of interests
The authors declare that they have no known competing financial interests or personal relationships that could have appeared to influence the work reported in this paper.
The authors declare the following financial interests/personal relationships which may be considered as potential competing interests

Supplementary data

Supplementary material

REFERENCES

1. Edidin M. Lipids on the frontier: a century of cell-membrane bilayers. Nat Rev Mol Cell Biol.

2. Steinmark IE, James AL, Chung PH, Morton PE, Parsons M, Dreiss CA, et al. Targeted fluorescence lifetime probes reveal responsive organelle viscosity and membrane fluidity. PLoS One. 2019;14: e0211165.

3. Kuimova MK. Mapping viscosity in cells using molecular rotors. Phys Chem Chem Phys. 2012;14: 12671-12686.

4. Benniston AC. Monitoring Rheological Properties in Biological Systems by Fluorescence Spectroscopy using Borondipyrromethene (Bodipy) Dyes: A Mini Review. J Anal Bioanal Tech. 2014;5: 1000221.

5. Kottas GS, Clarke LI, Horinek D, Michl J. Artificial molecular rotors. Chem Rev. 2005;105: 1281-1376.

6. Haidekker MA, Theodorakis EA. Environment-sensitive behavior of fluorescent molecular rotors. J Biol Eng. 2010;4: 11.

7. Kuimova MK, Yahioglu G, Levitt JA, Suhling K. Molecular rotor measures viscosity of live cells via fluorescence lifetime imaging. J Am Chem Soc. 2008:130: 6672-6673.

8. Lopez-Duarte I, Vu TT, Izquierdo MA, Bull JA, Kuimova MK. A molecular rotor for measuring viscosity in plasma membranes of live cells. Chem Commun. 2014;50: 5282-5284.

9. Wu Y, Štefl M, Olzyńska A, Hof M, Yahioglu G, Yip P, et al. Molecular rheometry: direct determination of viscosity in Lo and Ld lipid phases via fluorescence lifetime imaging. Phys Chem Chem Phys. 2013;15: 14986-14993.

10. Vyšniauskas A, Qurashi M, Gallop N, Balaz M, Anderson HL, Kuimova MK. Unravelling the effect of temperature on viscosity-sensitive fluorescent molecular rotors. Chem Sci. 2015;6: 5773-5778.

11. Saffman PG, Delbrück M. Brownian motion in biological membranes. Proc Natl Acad Sci USA. 1975;72: 3111-3113.

moving in a membrane. J Fluid Mech. 1981;110: 349-372.

13. Petrov EP, Schwille P. Translational diffusion in lipid membranes beyond the Saffman-Delbruck approximation. Biophys J. 2008;94: L41-L43.

14. Manzo C, Garcia-Parajo MF. A review of progress in single particle tracking: from methods to biophysical insights. Rep Prog Phys. 2015;78: 124601.

15. Haustein E, Schwille P. Fluorescence correlation spectroscopy: novel variations of an established technique. Annu Rev Biophys Biomol Struct. 2007;36: 151-169.

16. Rayan G, Guet J-E, Taulier N, Pincet F, Urbach, W. Recent applications of fluorescence recovery after photobleaching (FRAP) to membrane bio-macromolecules. Sensors. 2010;10: 5927-5948.

17. Pincet F, Adrien V, Yang R, Delacotte J, Rothman JE, Urbach W. et al. FRAP to Characterize Molecular Diffusion and Interaction in Various Membrane Environments. PLoS One. 2016;11: e0158457.

18. Honerkamp-Smith AR, Woodhouse FG, Kantsler V, Goldstein. RE. Membrane Viscosity Determined from Shear-Driven Flow in Giant Vesicles. Phys Rev Lett. 2013;111: 038103.

19. Dimova R, Dietrich C, Hadjiisky A, Danov KB. Pouligny B. Falling ball viscometry of giant vesicle membranes: Finite-size effects. Eur Phys J B. 1999;12: 589-598.

20. Hormel TT, Kurihara SQ, Brennan MK, Wozniak MC, Parthasarathy R. Two-Point Microrheology of Phase-Separated Domains in Lipid Bilayers. Biophys J. 2015;109: 732-736.

21. Steinmark IE, Chung P-H, Ziolek RM, Cornell B, Smith P, Levitt JA, et al. Time-Resolved Fluorescence Anisotropy of a Molecular Rotor Resolves Microscopic Viscosity Parameters in Complex Environments. Small. 2020;16: 1907139.

22. Sakuma Y, Imai M, Yanagisawa M, Komura S. Adhesion of binary giant vesicles containing negative spontaneous curvature lipids induced by phase separation. Eur Phys J E. 2008;25: 403-

23. Petrov EP, Petrosyan R, Schwille P. Translational and rotational diffusion of micrometer-sized solid domains in lipid membranes. Soft Matter. *2012;*8: 7552-7555.

24. Levitt JA, Kuimova MK, Yahioglu G, Chung P-H, Suhling K, Philips D. Membrane-Bound Molecular Rotors Measure Viscosity in Live Cells via Fluorescence Lifetime Imaging. J Phys Chem C. 2009;113: 11634-11642.

25. Koronakis V, Eswaran J, Hughes C. Structure and Function of TolC: The Bacterial Exit Duct for Proteins and Drugs. Annu Rev Biochem. 2004;73: 467-489.

26. Daury L, Orange F, Taveau J-C, Verchère A, Monlezun L, Gounou C, et al. Tripartite assembly of RND multidrug efflux pumps. Nat Commun. 2016;7: 10731.

27. Angelova MI, Dimitrov DS. Liposome electroformation. Faraday Discuss. Chem. Soc. 1986;81: 303-311.

28. Angelova MI, Soléau S, Méléard P, Faucon F, Bothorel P. Preparation of giant vesicles by external AC electric fields. Kinetics and applications. Progr Colloid Polym Sci. 1992:89: 127-131.

29. Aimon S, Manzi J, Schmidt D, Larrosa JAP, Bassereau P, Toombes GES. Functional reconstitution of a voltage-gated potassium channel in giant unilamellar vesicles. PLoS One. 2011;6: e25529.

30. Becker W, Bergmann A, Hink MA, König K, Benndorf K, Biskup C. Fluorescence lifetime imaging by time-correlated single-photon counting. Microsc Res Tech. 2004;63: 58-66.

31. Motta I, Gohlke A, Adrien V, Li F, Gardavot H, Rothman JE, et al. Formation of Giant Unilamellar Proteo-Liposomes by Osmotic Schock. Langmuir. 2015;31: 7091-7099.

32. Dent MR, López-Duarte I, Dickson CJ, Geoghegan ND, Cooper JM, Gould IR, et al. Imaging phase separation in model lipid membranes through the use of BODIPY based molecular rotors. Phys Chem Chem Phys. 2015;17: 18393-18402.

time-domain fluorescence lifetime imaging microscopy: practical application to protein-protein interactions using global analysis. J R Soc Inetrface. 2009;6: S93-S105.

34. Hosny NA, Mohamedi G, Rademeyer P, Owen J, Wu Y, Tang M-X, et al. Mapping microbubble viscosity using fluorescence lifetime imaging of molecular rotors. Proc Natl Acad Sci USA. 2013;110: 9225-9230.

35. Hosny NA, Fitzgerald C, Tong C, Kalberer M, Kuimova MK, Pope FD. Fluorescent lifetime imaging of atmospheric aerosols: a direct probe of aerosol viscosity. Faraday Discuss. 2013;165: 343-356.

36. Förster T, Hoffmann G. Die Viskositätsabhängigkeit der Fluoreszenzquantenausbeuten einiger Farbstoffsysteme. Z Phys Chem Neue Fol. 1971;75: 63-76.

37. Mullineaux CW, Kirchhoff H. Using Fluorescence Recovery After Photobleaching to Measure Lipid Diffusion in Membranes. In: Dopico AM, Editors. Methods in Membrane Lipids. Methods in Molecular Biology. Totowa: Humana Press; 2007. pp. 267-275.

38. Soumpasis DM. Theoretical analysis of fluorescence photobleaching recovery experiments. Biophys J. 1983;41: 95-97.

39. den Otter WK, Shkulipa SA. Intermonolayer Friction and Surface Shear Viscosity of Lipid Bilayer Membranes. Biophys J. 2007;93: 423-433.

40. Shkulipa SA, den Otter WK, Briels WJ. Surface Viscosity, Diffusion, and Intermonolayer Friction: Simulating Sheared Amphiphilic Bilayers. Biophys J. 2005;89: 823-829.

41. Espinosa G, López-Montero I, Monroy F, Langevin D. Shear rheology of lipid monolayers and insights on membrane fluidity. Proc Natl Acad Sci USA. 2011;108: 6008-6013.

42. Filipe HAL, Moreno MJ, Loura LMS. The Secret Lives of Fluorescent Membrane Probes as Revealed by Molecular Dynamics Simulations. Molecules. 2020;25: 3424.

43. Suhaj A, Le Marois A, Williamson DJ, Suhling K, Lorenz CD, Owen DM. PRODAN

44. Ariola FS, Li Z, Cornejo C, Bittman R, Heikal AA. Membrane fluidity and lipid order in ternary giant unilamellar vesicles using a new bodipy-cholesterol derivative. Biophys J. 2009;96: 2696-2708.

45. Filippov A, Orädd G, Lindblom G. Influence of Cholesterol and Water Content on Phospholipid Lateral Diffusion in Bilayers. Langmuir. 2003;19: 6397-6400.

46. Przybylo M, Sýkora J, Humpoličková J, Benda A, Zan A, Hof M. Lipid Diffusion in Giant Unilamellar Vesicles is More than 2 Time Faster than in Supported Phospholipid Bilayers under Identical Conditions. Langmuir. 2006;22: 9096-9099.

47. Heinneman F, Betaneli V, Thomas FA, Schwille P. Quantifying Lipid Diffusion by Fluorescence Correlation Spectroscopy: A Critical Treatise. Langmuir. 2012;28: 13395-13404.

48. Kahya N, Schwille P. How Phospholipid-Cholesterol Interactions Modulate Lipid Lateral Diffusion, as Revealed by Fluorescence Correlation Spectroscopy. J Fluoresc. 2006;16: 671-678.

49. http://lipid.phys.cmu.edu/papers16/SummaryTable8-21-17.ppt

50. Avanti Polar Lipids, Phase Transition Temperatures for Glycerophospholipids. https://avantilipids.com/tech-support/physical-properties/phase-transition-temps

51. Galla HJ, Hartmann W, Theilen U, Sackmann E. On two-dimensional passive random walk in lipid bilayers and fluid pathways in biomembranes. J Membrane Biol. 1979;48: 215-236.

52. Derzko Z, Jacobson K. Comparative lateral diffusion of fluorescent lipid analogs in phospholipid multibilayers. Biochemistry. 1980;19: 6050-6057.

53. Horner A, Akimov SA, Pohl P. Long and short lipid molecules experience the same interleaflet drag in lipid bilayers. Phys Rev Lett. 2013;110: 268101.

54. Lu D, Vavasour I, Morrow MR. Smoothed acyl chain orientational order parameter profiles in dimyristoylphosphatidylcholine-distearoylphosphatidylcholine mixtures: a 2H-NMR study.

55. Goutaland Q, Fournier JB. Saffman-Delbrück and beyond: A pointlike approach. Eur Phys J E. 2019;42: 156.

56. Xu ZC, Cafiso DS. Phospholipid packing and conformation in small vesicles revealed by two-dimensional 1H nuclear magnetic resonance cross-relaxation spectroscopy. Biophys J. 1986; 49: 779-783.

57. Kučerka N, Nagle JF, Sachs JN, Feller SE, Pencer J, Jackson A. et al. Lipid Bilayer Structure Determined by the Simultaneous Analysis of Neutron and X-Ray Scattering Data. Biophys J. 2008:95: 2356-2367.

58. Quemeneur F, Sigurdsson JK, Renner M, Atzberger PJ, Bassereau P, Lacoste D. Shape matters in protein mobility within membranes. Proc Natl Acad Sci USA. 2014;111: 5083-5087.

59. Almeida PFF, Vaz WLC. Lateral Diffusion in Membranes. In: Lipowsky R, Sackmann E, Editors. Structure and Dynamics of Membranes: From Cells to Vesicles. Handbook of Biological Physics. Volume 1. Amsterdam: Elsevier. 1995. pp. 305-357.

60. Busch S, Smuda C, Pardo LC, Unruh T. Molecular Mechanism of Long-Range Diffusion in Phospholipid Membranes Studied by Quasielastic Neutron Scattering. J Am Chem Soc. 2010;132: 3232-3233.

61. Gambin Y, Lopez-Esparza R, Reffay M, Sierecki N, Gov NS, Genest M, et al. Lateral mobility of proteins in liquid membranes revisited. Proc Natl Acad Sci USA. 2006;103: 2098-2102.

62. Apajalahti T, Niemelä P, Govindan PN, Miettinen MS, Salonen E, Marrink SJ, et al. Concerted diffusion of lipids in raft-like membranes. Faraday Discuss. 2010;144: 411-430.

63. Du D, Wang Z, James NR, Voss JE, Klimont E, Ohene-Agyei T, et al. Structure of the AcrAB-TolC multidrug efflux pump. Nature. 2014;509: 512-515.

64. Phan G, Benabdelhak H, Lascombe MB, Benas P, Rety S, Picard M, et al. Structural and

2010;18: 507-517.

65. Niemelä PS, Miettinen MS, Monticelli L, Hammaren H, Bjelkmar P, Murtola. T, et al. Membrane Proteins Diffuse as Dynamic Complexes with Lipids. J Am Chem Soc. 2010;132: 7574-7575.

66. Perez J, Koutsioubas A. Memprot: a program to model the detergent corona around a membrane protein based on SEC-SAXS data. Acta Cryst D. 2015;71: 86-93.

67. Koutsioubas A, Berthaud A, Mangenot S, Pérez J. Ab Initio and All-Atom Modeling of Detergent Organization Around Aquaporin-0 Based on SAXS Data. J Phys Chem B. 2013;117: 13588-13594.

68. Lindsey H, Petersen NO, Chan SI. Physicochemical characterization of 1,2-diphytanoyl-sn-glycero-3-phosphocholine in model membrane systems. Biochim Biophys Acta. 1979:555: 147-167.

69. Biltonen RL, Lichtenberg D. The use of differential scanning calorimetry as a tool to characterize liposome preparations. Chem Phys Lipids. 1993;64:129-142.

70. Wang S, Larson RG. Water channel formation and ion transport in linear and branched lipid bilayers. Phys Chem Chem Phys. 2014;16: 7251-7262.

71. Vaz WLC, Hallmann D. Experimental evidence against the applicability of the Saffman-Delbrück model to the translational diffusion of lipids in phosphatidylcholine bilayer membranes. FEBS Letters. 1983;152: 287-290.

72. Cybulski L.E, de Mendoza D. Bilayer Hydrophobic Thickness and Integral Membrane Protein Function. Curr Protein Pept Sci. 2011;12: 760–766.

73. Marguet D, Salomé L. Lateral Diffusion in Heterogeneous Cell Membranes. In: Bassereau P, Sens P, Editors. Physics of Biological Membranes. Cham: Springer: 2018. pp. 169–189.

74. Simunovic M, Voth G A, Callan-Jones A, Bassereau P. When Physics Takes Over: BAR

75. Naji A, Levine AJ, Pincus PA. Corrections to the Saffman-Delbrück Mobility for Membrane Bound Proteins. Biophys J. 2007;93: L49–L51.

76. Kreutzberger AJB, Ji M, Aaron J, Mihaljević L, Urban S. Rhomboid Distorts Lipids to Break the Viscosity-Imposed Speed Limit of Membrane Diffusion. Science. 2019;363(6426): eaao0076.

77. Henle ML, Levine AJ. Effective viscosity of a dilute suspension of membrane-bound inclusions. Phys Fluids. 2009;21: 033106.

78. Seddon AM, Casey D, Law RV, Gee A, Templer RH, Ces O. Drug interactions with lipid membranes. Chem Soc Rev. 2009;38: 2509-2519.

79. Klymchenko AS, Duportail G, Demchenko AP, Mély Y. Bimodal distribution and fluorescence response of environment-sensitive probes in lipid bilayers. Biophys J. 2004;86: 2929–2941.

80. Burns AR, Frankel DJ, Buranda T. Local mobility in lipid domains of supportedbilayers characterized by atomic force microscopy and fluorescence correlation spectroscopy. Biophys J. 2005;89: 1081–1093.

81. Israelachvili JN. Measurement of the viscosity of liquids in very thin films. J Colloid Interface Sci. 1986;110: 263-271.

82. Polita A, Toliautas S, Žvirblis R, Vyšniauskas A. The effect of solvent polarity and macromolecular crowding on the viscosity sensitivity of a molecular rotor BODIPY-C_{10}. Phys Chem Chem Phys. 2020;22: 8296-8303.

Graphical abstract

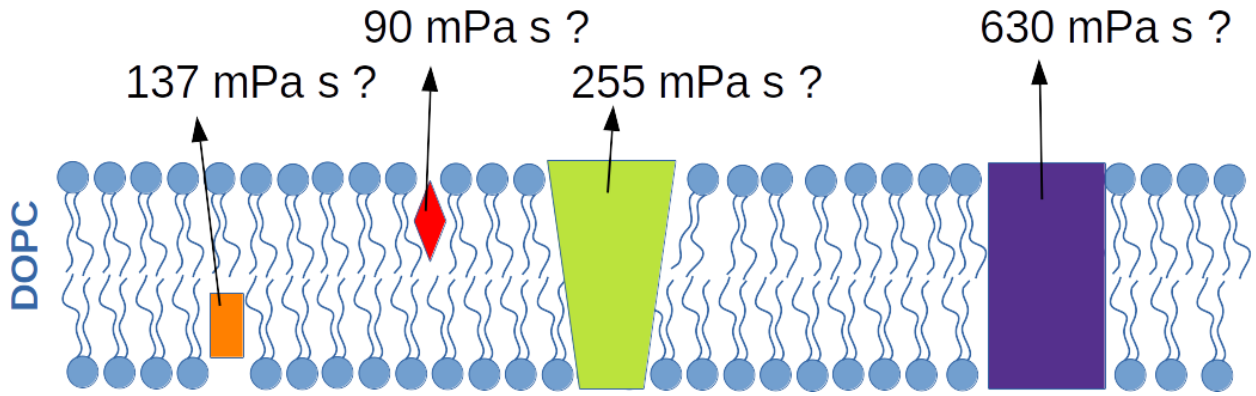

Highlights

- FLIM measurements most likely do not report the exact bilayer viscosity.
- Molecular probes in FRAP lead to erroneous viscosity values
- Micrometric-sized probes in FRAP lead to correct viscosity values.